# THE EFFECT OF LAND-SEA CONTRAST ON INTERANNUAL VARIABILITY OF THE ASIAN MONSOON*

*LUO Huibang* (罗会邦)

Department of Atmospheric Sciences, Zhongshan University, Guangzhou 510275

Received January 11, 1999; revised April 22, 1999

ABSTRACT

Values of the net radiative heating (*QRT*) at the top of atmosphere (TOA) are derived from the satellite-observed outgoing long wave radiation (*OLR*) and the TOA short wave net irradiance (*SHT*) for the region of the Tibetan Plateau and surrounding areas (40°S—40°N, 0—180°E) and the period of months from January 1979 to December 1988. The anomalous *QRT* (*QRTA*) in relation to the interannual variability of Asian monsoon is discussed. *QRTA* for the earth-atmosphere system in the domain may be linked to the thermal contrasts between continents and oceans and between the plateau and surrounding free atmosphere.

**Key words**: monsoon, interannual variation, land-sea contrast

## I. INTRODUCTION

In recent years some efforts (e.g., Yanai and Li 1994; Yang 1996) have been put into the topic on snow-monsoon-ENSO associations in order to provide better understanding of regional and global climate changes. Researches on monsoon-ENSO relationship (Yasunari 1991; Webster and Yang 1992; Huang and Fu 1993) concern the air-sea interaction, on the other hand, researches on snow-monsoon relationship (Barnett et al. 1989; Zhang et al. 1991; Li and Yanai 1991; Luo Huibang 1995; Chen et al. 1995) emphasize the role of land processes. Some investigators (Li 1987; Sun and Sun 1993; Luo Yong 1995) related the cold surge (winter monsoon) to the Aian summer monsoon/ENSO. Both ENSO and snow-cover/cold-surge are linked to the Asian summer monsoon variability.

It has long been recognized that the massive monsoon circulations in tropical and subtropical latitudes are driven by the seasonally reversing horizontal temperature gradients imposed upon the troposphere by the distribution of continents and oceans (Wallace and Hobbs 1977). From the above-mentioned snow-monsoon-ENSO associations, it is speculated that the interannaul variations of the monsoon circulations may also be influenced by the land-sea contrasts: the intensity of the thermal contrast changes in different years.

The purpose of this paper is to show that the net radiative heating (*QRT*) at the top of the atmosphere, i.e. the net thermal forcing on the upper boundary of the ocean-atmosphere-land system, can be used to describe the land-sea thermal contrast to a considerable degree. Moreover, it will be shown that the time variations of *QRT* are closely related to the

* The research is supported by "National Key Programme for Developing Basic Sciences" G 1998040900 Part I.

interannual variability of the Asian monsoon. In Section II, the data and analysis procedures are described. The horizontal distribution and the time variation of *QRT* are discussed in Sections III — V with efforts focused on the seesaw oscillation of anomalous *QRT* between continents and oceans on the interannual time scale. Section VI is devoted to the interannual relationship between *QRT* and the Asian monsoon. Conclusions and discussion are given in Section VII.

## II. DATA AND ANALYSIS PROCEDURES

As mentioned in the introduction, the net radiative heating at the top of the atmosphere, *QRT*, is used in this work. The reason for *QRT* to be chosen to study the interannual variation of the Asian monsoon is given in Appendix. *QRT* is computed by

$$QRT = SHT - OLR, \tag{1}$$

where *OLR* is the satellite-observed outgoing long wave radiation. *SHT* the short wave net irradiance at the top of the atmosphere. The data set analyzed in this study consists of monthly mean values of *OLR* and *SHT* in the domain of (40°S — 40°N, 0 — 180°E) for the period of 1979 — 1988. The monthly mean data are then used to examine the spatial and temporal variations of *QRT* in the Asian monsoon region and surrounding areas.

The main results of this paper are based on one-point correlation statistics and empirical orthogonal function analysis. These analysis methods have been extensively used and documented in many studies and need not be described here.

## III. HORIZONTAL DISTRIBUTION OF *QRT*

Figure 1 shows the distribution of the 10-year averaged *QRT*. It is seen from the figure that the large values of *QRT* are situated in equatorial areas due to larger values of *SHT* and smaller values of *OLR*. A positive center of *QRT* is also found over the Tibetan Plateau due to its high elevation, thus low surface temperatures and small values of *OLR*. On the other hand, negative centers of *QRT* are located over the desert areas due to higher surface temperature,

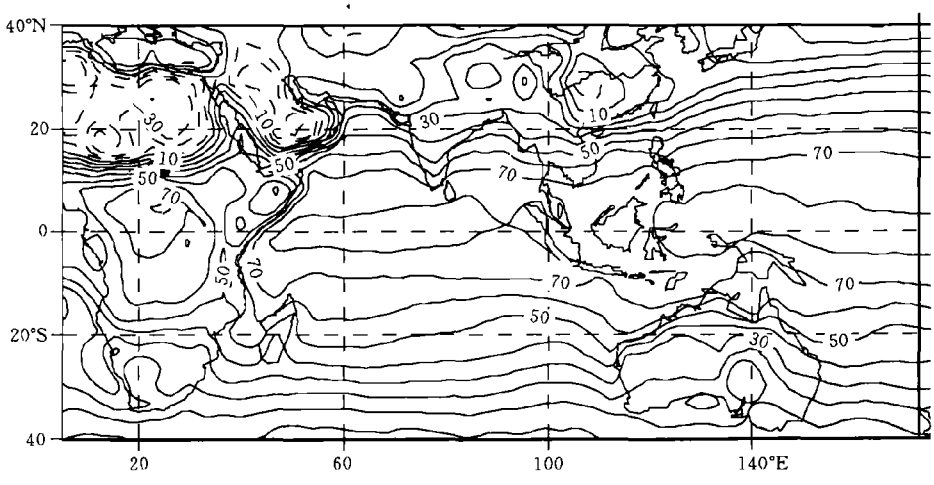


Fig. 1. 10-year mean *QRT*, 1979—1988, unit: W m$^{-2}$.

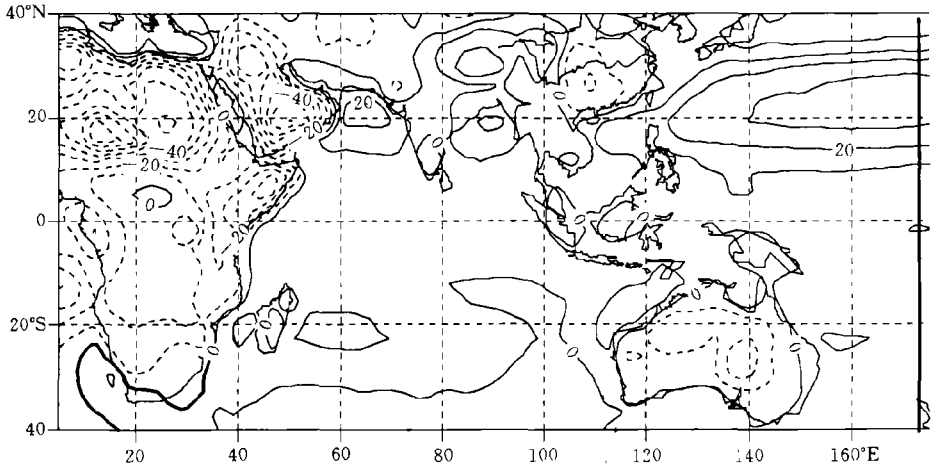


Fig. 2. Deviation of 10-year mean *QRT* from zonal mean (*QRTD*). Unit: W $m^{-2}$.

thus large values of *OLR*.

In order to reveal the effect of the land-sea contrast on the distribution of *QRT*, the deviation from latitudinal mean, *QRTD*, is computed and shown in Fig. 2. It can be seen from the figure that zero-contours (negative values are shown with dashed lines) almost coincide with coastal lines of Africa, Australia, Arabian Peninsula, etc. There exist positive values of *QRTD* in oceanic regions, and negative ones over continents except the Tibetan Plateau where sensible heat transport outward prevails. The positive (negative) values of *QRTD* over ocean (continent) may be mainly due to the fact that relatively oceanic region is the source region of sensible and latent heat, while the continent is the sink region (cf. Eq. (4) in Appendix). There exist negative values of *QRTD* over monsoon rain areas of India and China in summer (not shown) owing to the same reason.

## IV. ONE-POINT CORRELATION MAP OF *QRTA*

The temporal variations of *QRT* are discussed in this section. First the anomalies of the monthly mean *QRT* (hereafter referred to as *QRTA*) are computed as the deviation from their 10-year mean monthly values. To examine characteristics of interannual variations, standard deviations of *QRTA* are then computed. The results are plotted in Fig. 3. Large interannual variability is mostly confined in the subtropical oceanic regions of the Southern Hemisphere centered to the west of southern Africa and Australia. There also exists large interannual variablity in the region south of Yangtze (Changjiang) River and the western Tibetan Plateau.

Relationships of *QRTA* (the variations of *QRT*) in different regions are examined by computing correlation coefficients between all grid points in the analysis domain. Different grid points have been chosen as reference points, including standard deviation centers shown in Fig. 3, results in all cases show the same outstanding feature of seesaw oscillation between oceans and continents. Figure 4 presents the simultaneous correlations of *QRTA* between reference point of 30°N, 85°E and all other grid points (2.5°×2.5°) in the above-mentioned domain for 120-month period from January 1979 to December 1980. The zero correlation

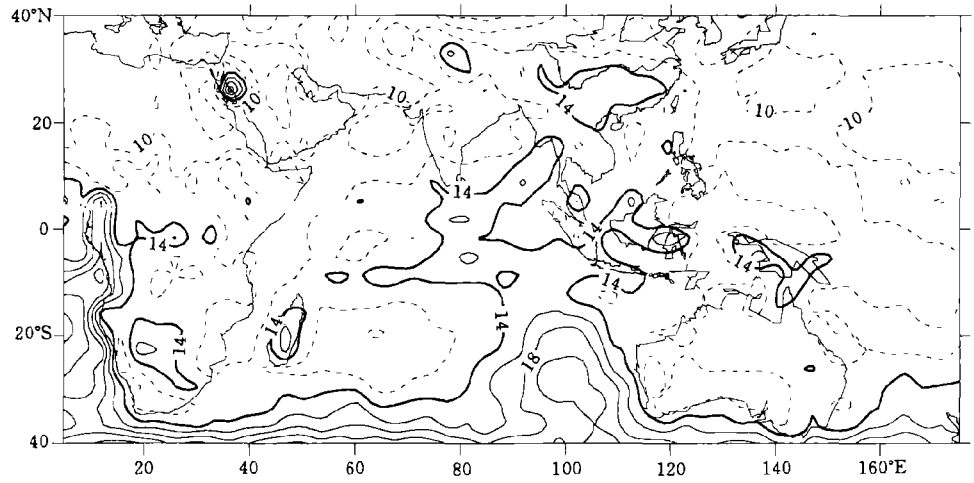


Fig. 3. Standard deviations of *QRTA*. Contour interval is 2 and regions larger than 14 are shaded.

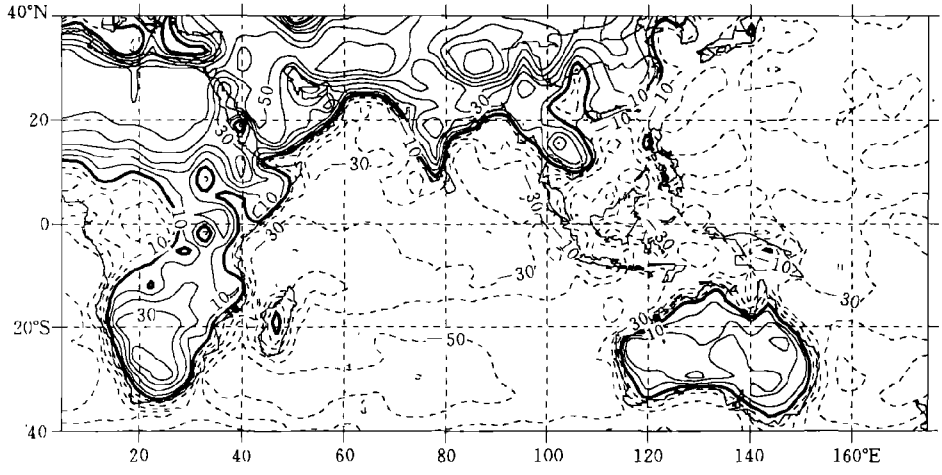


Fig. 4. Correlation map of *QRT* with reference point at 85°E, 30°N. Contours show correlation coefficients multiplied by 100.

coefficient contours also nearly depict the coastal lines of continents of Africa. Australia and Asia. This clearly shows the seesaw oscillation between continents and surrounding oceans.

To see the time scale of the seesaw oscillation, the time series of *QRTA* and their 13-month running mean at the grid points for the Tibetan Plateau and Mascarene are shown in Fig. 5. We see from this figure that the opposite sign relationship is clear except for the years 1987—1988 due to very small amplitude of the Mascarene time series during these two years. It is apparent that a 4-year quasi-periodic variation is present in the time series. The spectral analysis shows a key period of 43 months.

These features of the one-point correlation will be further examined by using EOF analysis

in the next section.

## V. EMPERICAL ORTHOGONAL FUNCTIONS (EOF) OF *QRTA*

To see how many percent of the total variance of the time series *QRTA* can be explained by the seesaw patterns, the EOF analysis is applied. Results are shown in Figs. 5—6 for the first and second eigenvectors (EOF1 and EOF2). EOF1 and EOF2 explain about 33% and 8%, respectively, of the total variance of the time series.

The land-ocean seesaw pattern found in the spatial structure of EOF1 (Fig. 6a) is a remarkable feature, which is rather like that obtained earlier from the one-point correlation map (Fig. 4). Positive anomalies are found mainly in oceanic areas, while negative ones over continents and even islands like Madagascar and Sumatra with centers located at desert and plateau areas. The solid line depicted in Fig. 7 represents the principal component time series for EOF1. It can be noted in Fig. 7 that the associated seesaw oscillation in EOF1 shows its largest amplitude in the time period around 1980—1981 similar to that for *QRTA* shown in Fig. 5.

The horizontal structure in EOF2 (Fig. 6b) is dominated by a north-south oriented wavy pattern to the east of 60°E and a rather complicated feature to the west. The positive anomaly is found in a band between 20°S—20°N stretching from the Indian Ocean into the western Pacific with negative one located to its south and north. But there exists a positive center over the Tibetan Plateau surrounded by negative anomaly areas. A noticeable feature is found in northwest part of the analysis domain, where positive centers alternating with negative ones on rather small scale. In the Northern Hemisphere, the above-mentioned features seem to be also influenced by the land-sea contrast and topography to some extent.

The anomalies are positive over the Tibetan Plateau and negative in the southern Indian Ocean in the one-point correlation map of *QRTA* (Fig. 4). The same opposite-sign anomaly distributions between the Tibetan Plateau and the southern Indian Ocean are observed also in

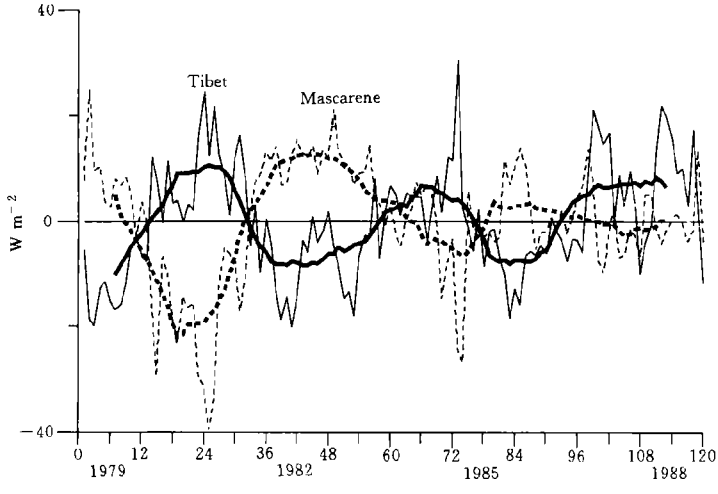


Fig. 5. Time series of *QRTA* over Tibet (solid) and Mascarene (dashed).

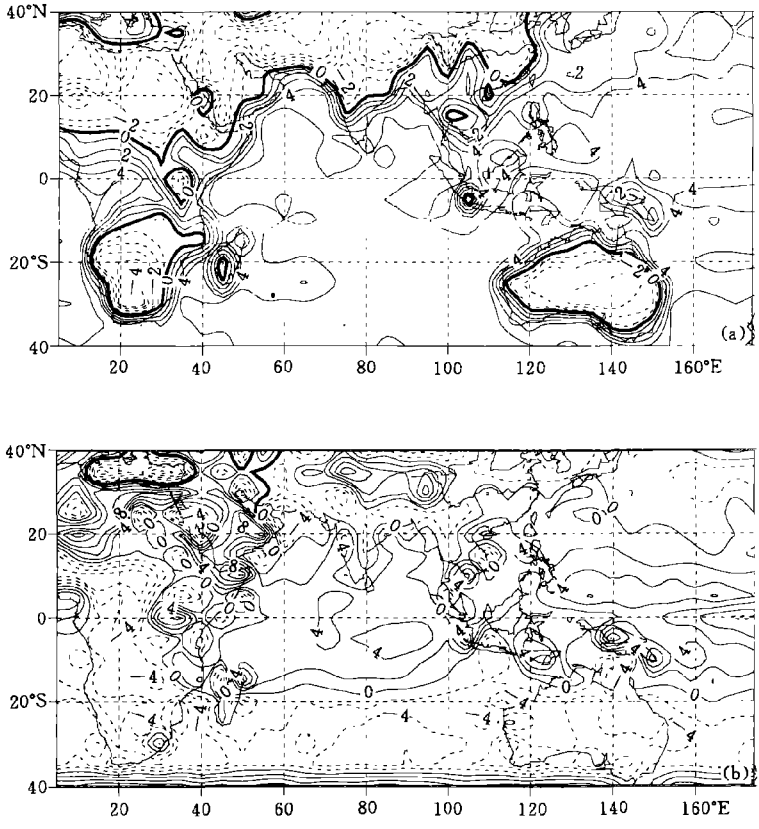


Fig. 6. Spatial structure of the EOF1 (a) and EOF2 (b). Contour values have been multiplied by 100.

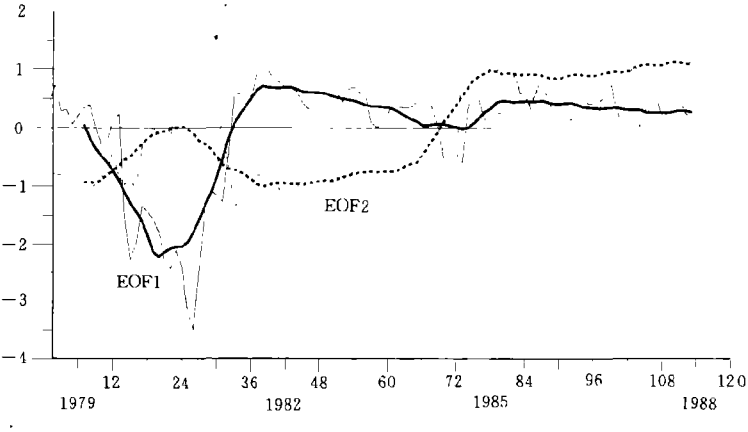


Fig. 7. The time series of EOF1 (solid) and EOF2 (dashed). Unit on ordinate has been divided by 10.

both EOF1 and EOF2. The time series for EOF2 is shown by the dashed line in Fig. 7. It is seen from Fig. 7 that the amplitude is very weak in the period of 1980 — 1981 when the

amplitude for EOF1 comes to its maximum. Thus, EOF1 contributes much to the seesaw oscillation. On the other hand, contribution from EOF2 is more important in the period from 1985 to 1988 (Fig. 7).

## VI. RELATIONSHIP BETWEEN THE INTERANNUAL VARIATION OF *QRTA* AND THE INTENSITY OF THE ASIAN MONSOON

It has been reviewed in the introduction section that the monsoon itself is governed by the land-sea thermal contrast. And it has been mentioned in Sections III—IV that the interannual variation in *QRTA* shows a seesaw oscillation pattern between continents and oceans, indicating the importance of land-sea contrasts. Thus the interannual variability of the monsoon may also be controlled by the land-sea contrast. The topic will be discussed in this section.

Li and Yanai (1996) listed four indices to measure the intensity of the Asian summer monsoon. Two of them were considered to represent the intensity of the broadscale monsoon circulation. The third one, the *OLR* index, was defined as the mean *OLR* averaged over South Asia, because the *OLR* flux can be used to define the intensity of convection associated with the summer monsoon. The last one is summer-month precipitation amounts averaged over the Indian subcontinent. They pointed out that the correlations among first three indices are fairly strong. Figure 8 shows the comparison of the *OLR* index and the time series of *QRTA* discussed in Section IV. The behaviors of *OLR* index and *QRTA* are found to be rather similar. *QRTA* is also correlated with the WY index although not so well as *OLR* index. Thus positive (negative) *QRTA* in the Tibetan Plateau (Mascarene) corresponds to active South Asian monsoon, and vise versa.

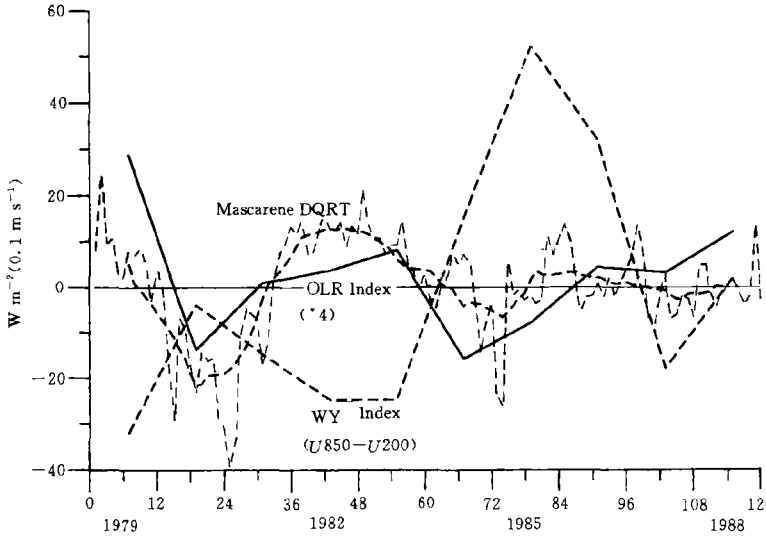


Fig. 8. Time series of summer mean anomaly of *OLR* index (solid) and WY index (thick dashed) (Li and Yanai 1996) and *ORTA* over Mascarene (dashed). 1979—1988.

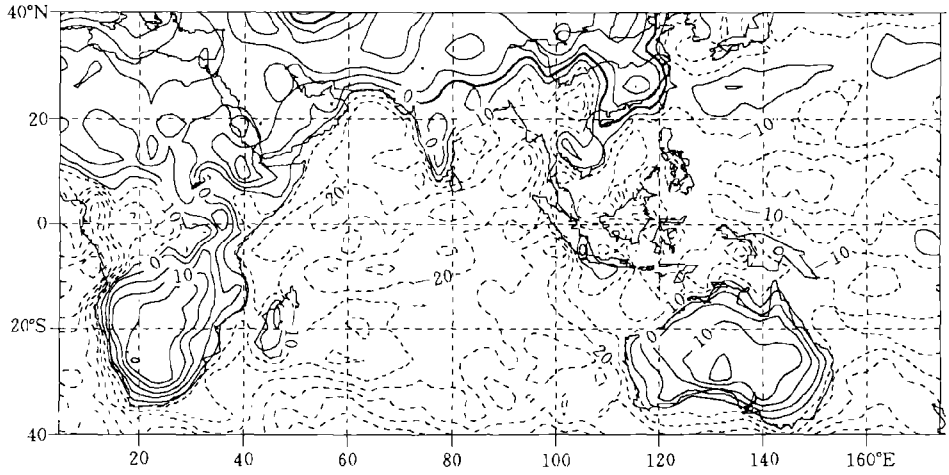


Fig. 9. The 12-month mean anomalies of *QRT*. 1980.

The year 1980 shows up as one of the strong monsoon years in both *OLR* index and *QRTA*. Figure 9 illustrates the distributions of the mean *QRTA* averaged in the year 1980. Compared to the one-point correlation map of *QRTA*, the common feature of positive anomalies over continents and negative ones over oceans is evident. Moreover, the structure pattern revealed in Fig. 9 is much similar to that in EOF1 (Fig. 6a) due to large amplitudes around 1980 for EOF1. As mentioned above, EOF1 is the major contributor to the interannual variation in *QRTA* during the time period around 1980.

Figure 8 reveals the close relationship between *QRTA* and monsoon intensity. Thus, *QRTA*-monsoon association provides us an alternative approach for the prediction of the Asian monsoon, the intensity of the summer monsoon may be inferred in preceding winter-spring in terms of the time series of monthly mean *QRTA*.

## VII. SUMMARY AND DISCUSSION

From above-discussed spatial and temporal variations of *QRT*, the major findings of this work are summarized as follows:

(1) The analyses of the horizontal distributions of the 120-month mean *QRTD* (deviation from zonal mean) for the period of 1979—1988 clearly reveal the dependence of *QRTD* on the land-sea contrast.

(2) The one-point correlation computations of the monthly mean *QRTA* (anomaly from 10-year mean) in the period from January 1979 to December 1988 for the region from 0° eastward to 180°E and from 40°S to 40°N show remarkable seesaw oscillation between oceans and continents with a key period of about 43 months.

(3) The seesaw oscillation is closely related to the interannual variation of the Asian summer monsoon. Positive (negative) *QRTA* in the Tibetan Plateau (Mascarene) region corresponds to active South Asian monsoon, and vise versa. Thus not only Asian monsoon itself but also its interannual variation is governed by the land-sea contrast.

(4) The intensity of the Asian summer monsoon may be predicted in preceding winter-

spring in terms of the time series of monthly mean $QRTA$ based on the close relationship between $QRTA$ and monsoon intensity.

It has bee demonstrated in this study that the variability of the Asian monsoon is closely associated with the variability of $QRTA$ which is influenced by the land-sea contrast. On the other hand, it can be seen from Eq. (4) in Appendix that $QRT$, the net radiative heating at the top of the atmosphere (i. e. the net thermal forcing on the upper boundary of the ocean-atmosphere-land system), is governed by the sensible and latent heat fluxes $\boldsymbol{F}_{AS}$, $\boldsymbol{F}_{O}$ and $\boldsymbol{F}_{AL}$ in the atmosphere and ocean from the climate system. And the fluxes $\boldsymbol{F}_{AS}$, $\boldsymbol{F}_{O}$ and $\boldsymbol{F}_{AL}$ and are closely related to the surface condition SST and snow-cover. This suggests that both land processes and the air-sea interaction are important for the dynamics of the monsoon climate. Thus the work on $QRT$-SST-snow associations needs to be done to provide better understanding of the interannual variability of the Asian monsoon and, moreover, the ENSO-snow-monsoon associations.

## APPENDIX: THE IMPLICATION OF $QRT$

Time-averaged thermodynamic equations for the atmosphere and for the ocean and the moisture balance equation for the atmosphere can be written respectively as

$$div\ \boldsymbol{F}\mathrm{AS} = QRT - QRS + HS + LP, \tag{1}$$

$$div\ \boldsymbol{F}_{O} = QRS - HS - LE, \tag{2}$$

$$div\ \boldsymbol{F}_{AL} = -L(P - E), \tag{3}$$

where $QRT$ and $QRS$ are the net radiative energy fluxes per unit area at the top and surface, $P$ and $E$ the amounts of precipitation and evaporation per unit area at the surface, $\boldsymbol{F}_{AS}$ and $\boldsymbol{F}_{O}$ the horizontal sensible heat fluxes per unit area in the atmosphere and ocean respectively; $\boldsymbol{F}_{AL}$ is the horizontal latent heat flux per unit area in the atmosphere, $div$ the notation for the divergence, $L$ the latent heat of condensation, $HS$ the sensible heat flux per unit area at the surface.

Adding (1), (2) and (3) yields

$$div\ (\boldsymbol{F}_{AS} + \boldsymbol{F}_{O} + \boldsymbol{F}_{AL}) = QRT. \tag{4}$$

Considering storage terms, (4) can be written as

$$div\ (\boldsymbol{F}_{AS} + \boldsymbol{F}_{O} + \boldsymbol{F}_{A:}) = QRT - (S_{AS} + S_{AL} + S_{O} + S_{LD}). \tag{5}$$

The last term on the right-hand side of (5) stands for the storage of heat amount in atmosphere, ocean and land.

It can be seen by integrating (4) horizontally for a region that the transport of sensible (latent) heat outward (inward) from the region for the long-term mean is governed by $QRT$, i. e. the net thermal forcing on the upper boundary of the region. For example, if the monsoon rain region is taken as the domain, then inflow (outflow) of the latent heat corresponds to negative (positive) $QRT$. Thus anomalous $QRT$ can be used to describe the variability of the monsoon rainfall. Moreover, the satellite-observed data may be the only valid data for researches on meteorology over a large domain including mountainous and oceanic areas. These are the reasons for $QRT$ to be chosen to study the interannual variation of the Asian monsoon.

## REFERENCES

Barnett, T. P., Dumenil, L., Schlese, U., Roeckner, E. and Latif, M. (1989). The effect of Eurasian snow cover on regional and global climate variations. *J. Atmos. Sci.*, **46**: 661—685.

Chen Longxun, Miao Qun and Niu Tao (1995). Impact of Tibetan snow cover on the general circulation of atmosphere in Asia, International Workshop on TIPEX (IWTE-1), pp. 119—122, Beijing, China.

Huang Ronghui and Fu Y. (1993). Impact of Asian monsoon on the ENSO event. Proc. of the Seventh Japan and East China Seas Study/Pacific Marginal Seas Workshop, May, 9—15, Qingdao, China.

Li Chongyin. (1987). A study on interaction between general circulation in East Asia an El Nino. *Atmos. Sci. Sin.*, **11**: 359—364 (in Chinese).

Li, C. and Yanai, M. (1996). The onset and interannual variability of the Asian summer monsoon in relation to land-sea thermal contrast. *J. Climate*, **9**: 358—375.

Luo Huibang (1995). Effect of winter monsoon on summer monsoon through air-sea interaction. *Acta Meteor. Sinica*, **9**: 26—34.

Luo Yong (1995). A study on winter-spring snow cover over Qinghai-Xizang Plateau and its effect on summer circulations in East Asia. *Plateau Meteor.*, **14**: 505—512 (in Chinese).

Sun Bomin and Sun Shuqing (1993). The features of global atmospheric circulation in preceding winter for the summer drought or flooding in the Changjiang River Valley in China. The 5th RC-US Monsoon Workshop. 21—22, Hangzhou, China.

Wallace, J. M. and Hobbs, P. V. (1977). Atmospheric Sciences. pp. 467. Academic Press. New York. San Francisco. London.

Webster, P. J. and Yang, S. (1992). Monsoon and ENSO electively inteactive systems. *Quart. J. Meteor. Soc.*, **118**: 877—926.

Yanai, M. and Li, X. (1994). Interannual variability of the Asian summer monsoon and its relationship with ENSO, Eurasian snowcover and heating. Proc. International Conference on Monsoon Variability and Prediction, pp. 27—34. Trieste, Italy.

Yang, S. (1996). ENSO-snow-monsoon associations and seasonal-interannual predictions. *Intern. J. Climatology*, **16**: 1—10.

Yasunari, T., (1991). The monsoon year—A new concept of the climatic year in the tropics. *Bull. Amer. Meteor. Soc.*, **72**: 1331—1338.

Zhang Zhengqiu, Li Weiliang and Chen Longxun (1991). Numerical experiments on the effect of Qinghai-Xizang Plateau snow cover on summer monsoon formation. *Acta Meteor. Sinica*, **5**: 442—455.